Astronomy & Astrophysics manuscript no. Sausage˙mode˙1i
November 16, 2011
© ESO 2011

Intensity variations associated with fast sausage modes

M. Gruszecki,[1] V. M. Nakariakov,[1,2] T. Van Doorsselaere[3,4]

[1] Centre for Fusion, Space and Astrophysics, Department of Physics, University of Warwick, Coventry CV4 7AL, United Kingdom
[2] Central Astronomical Observatory at Pulkovo of the Russian Academy of Sciences, 196140 St Petersburg, Russia
[3] Centrum voor Plasma-Astrofysica, Mathematics Department, KULeuven, Celestijnenlaan 200B bus 2400, 3001 Leuven, Belgium
[4] Post-doctoral researcher of the FWO-Vlaanderen

received / accepted

ABSTRACT

Aims. We determine the dependence of the observed properties of fast magnetoacoustic axisymmetric oscillations (the sausage mode) of a thick and dense flaring coronal loop, modelled by a magnetic cylinder, on the parameters of the equilibrium plasma configuration. The plasma inside and outside the cylinder is of low-beta, and penetrated by a straight magnetic field. The plasma density has a smooth profile across the magnetic field.
Methods. We use 3D ideal magnetohydrodynamic equations to model numerically the development of the perturbations of the cylindrical equilibrium, considering both leaky and trapped regimes.
Results. Short-period sausage oscillations, trapped by the cylinder, are qualitatively consistent with the analytical results obtained in the models of a plasma slab or a cylinder with a step-function transverse profile. The period of trapped sausage oscillations is determined by the ratio of the phase speed, with the value between the internal and external Alfvén speeds, and the wavelength. Longer-period sausage oscillations are leaky, with the decay time longer for higher density contrast between the internal and external media. Leaky sausage oscillations have longer periods than trapped sausage oscillations of the same cylinder. In the coronal conditions, sausage oscillations are essentially compressible and transverse, and hence produce modulation of the thermal optically-thin emission intensity and periodic Doppler broadening of emission lines. However, if the oscillating plasma non-uniformity is poorly spatially resolved, the variation of the emission intensity is weak, proportional to the actual amplitude of the oscillation squared. The latter effect is connected with the transverse nature of the oscillation, causing the conservation of mass in the transverse cross-section of the oscillating plasma structure.

Key words. Magnethydrodynamics (MHD) – Sun: solar corona

1. Introduction

The magnetically dominated plasma of the solar corona is an elastic and compressible medium that can support propagation of magnetohydrodynamic (MHD) waves. Structuring of the physical parameters of the corona affect dramatically the properties of the waves, which must be taken into account in the interpretation of observed phenomena. A popular model for the study of the effect of structuring on MHD waves is a straight plasma cylinder, representing, e.g. a segment of a coronal loop, prominence tread, plasma jet, plume, etc. In particular, a cylinder of dense plasma penetrated by the magnetic field parallel to the axis of the cylinder, and surrounded by a plasma with different density and temperature with a different value of the magnetic field, can support propagation of MHD modes, which are collective perturbations of the internal and external plasma media (e.g. Nakariakov & Verwichte 2005).

The properties of the MHD modes are determined, in particular, by the azymuthal wave number m. The axisymmetric **fast mode** perturbations with $m = 0$ are known as the sausage (or radial, or peristaltic) mode. Studies of this mode have attracted attention for many years (Rosenberg 1970; Zaitsev & Stepanov 1975; Roberts et al. 1984; Cally 1986). This mode is a symmetric perturbation of the cross-section of a plasma non-uniformity, which does not perturb the axis of the loop. The sausage mode is essentially compressible, with the density perturbations in phase with the perturbations of the magnetic field and in anti-phase with the perturbations of the loop minor radius. In a low-β plasma, typical for solar coronal active regions, the plasma motions induced by the sausage mode are almost perpendicular to the axis of the cylinder. There is also a slow magnetoacoustic mode of the same symmetry, $m = 0$, referred to as a slow sausage mode.

Observationally, the sausage mode was identified in the microwave and hard X-ray emission produced by flaring coronal loops (Nakariakov et al. 2003; Melnikov et al. 2005; Inglis et al. 2008), and also in H_α emission from cool, post-flare loops (Srivastava et al. 2008). Due to very short periods (1-10 s) the observations require high time-resolution instruments. The first spatially resolved detection of a sausage mode was made by Nakariakov et al. (2003) with the Nobeyama Radioheliograph. They found in-phase variation of the 17 GHz and 34 GHz emission along a thick and short flaring loop, which had a well pronounced spectral peak near 17 s. The oscillatory signal was strongest at

Send offprint requests to: M. Gruszecki e-mail: M.Gruszecki@warwick.ac.uk

the loop top and had minima near the footpoints. It was concluded that the fundamental (or global) sausage mode of the flaring loop was detected. The more detailed studies of Melnikov et al. (2005) confirmed that conclusion. The interest in the coronal fast sausage modes is connected with the possibility for the seismological estimate of the external magnetic field in the oscillating plasma non-uniformity, and also with the possible role played by this mode in the acceleration of non-thermal particles and their dynamics (see, e.g. Zaitsev & Stepanov 1982; Brown & Hoyng 1975). Also, Fujimura & Tsuneta (2009) reported a sausage mode of the photospheric magnetic flux tube, with the period in the range from 3 to 6 minutes, observed with Hinode/SOT. Van Doorsselaere et al. (2011) have used the detection of the fast sausage mode and a slow mode in a flare to measure the local plasma-β.

The theoretical studies of the sausage mode of a plasma cylinder were performed in terms of the dispersion relation formalism (Zaitsev & Stepanov 1975; Edwin & Roberts 1982; Roberts et al. 1984; Cally 1986; Kopylova et al. 2007). It was pointed out that, depending upon the ratio of the wavelength to the radius of the cylinder, there are two possible regimes, trapped and leaky. Trapped modes are confined to the cylinder, while leaky modes radiate the energy into the external medium. For the typical coronal conditions ($\beta \ll 1$) trapped sausage modes exist when the external Alfvén speed C_{Ae} exceeds the value of the internal Alfvén speed C_{Ai}. Despite both fast and slow magnetoacoustic oscillations can be of the sausage symmetry, the term "sausage" is usually applied to the fast mode. (Slow sausage modes are usually referred to as "longitudinal", as in the coronal conditions they practically do not perturb the radius of the cylinder).

The phase speed of the trapped sausage mode is between the Alfvén speed values inside C_{Ai} and outside C_{Ae} the plasma structure. In a low-β plasma, the condition $C_{Ai} < C_{Ae}$ is usually connected with the enhanced density of the plasma inside the wave-guiding structure. The decrease in the wave number leads to the increase in the phase speed up to the external Alfvén speed, where the mode is subject to a cut-off. For wave numbers smaller than the cut-off value, sausage modes become leaky, by the violation of the total internal reflection condition. Additional leakage can be associated with the loop curvature, (see, e.g. Verwichte et al. 2006), but we do not consider this mechanism in this study. The cut-off value for the wave number decreases with the increase in the density contrast between the internal and external media (see, e.g. Roberts et al. 1984). In numerical studies in the zero-β limit, Pascoe et al. (2007b) showed the existence of leaky global sausage modes in the case of long loops with small density contrasts. The period of the leaky global sausage mode was found to be almost independent of the internal Alfvén speed C_{Ai} and determined by the Alfvén speed outside the loop C_{Ae}. Additionally, it was shown that the period of the global sausage mode of a thick and dense plasma cylinder, **typical e.g. for a flaring coronal loop,** was determined by the loop length L (Nakariakov et al. 2003; Aschwanden et al. 2004). Numerical studies of Pascoe et al. (2007a, 2009) confirmed that this result is not sensitive to internal structuring of the oscillating cylinder, and to the variation of its cross-sectional area in the longitudinal direction. Also, Inglis et al. (2009) confirmed results obtained by Pascoe et al. (2007b) for finite plasma β and additionally showed that the period of the global sausage mode is not significantly affected by finite values of β, with the variation remaining less than 5% for a broad range of plasma parameters. The latter statement is applied to the normalised value of the period, when the effect of the modification of the equilibrium values was not considered. **Thus, it was concluded that the period of sausage oscillations of typical flaring loops, with the large aspect ratio of the minor radius to the length, is determined by the loop length rather than its minor radius.**

The use of the slab model instead of the cylinder for the study of sausage oscillations is usually justified by the apparent consistency of the analytical results obtained in those geometries in the trapped regime (Edwin & Roberts 1983; Roberts et al. 1984). However, there is a significant difference in the behaviour of the waves outside the plasma non-uniformity in the Cartesian and cylindrical geometries, pointed out by, e.g. (Díaz et al. 2004). The aim of this paper is to study ***observational*** *properties of trapped and leaky sausage modes* of a thick and dense flaring loop in the thermal, optically-thin emission, accounting for the effects of cylindrical geometry. Properties of the sausage mode are studied by direct numerical simulations **of the initial value problem,** with the use of the full set of ideal MHD equations, in the 3D geometry. We choose a cylinder with smooth radial (transverse) profiles of the equilibrium physical quantities. In contrast with the case of a plasma slab, which allows for a simple analytical solution of the linear problem in the case of the zero-β plasma for a symmetric Epstein profile (see, e.g. Cooper et al. 2003b), in the cylindrical geometry analytical solutions are known for the step-function transverse profiles only (Edwin & Roberts 1983). However, even in this case, the analytical study of leaky modes is rather non-trivial, as it requires careful treatment of different branches of Bessel functions of a complex argument (see Ruderman & Roberts 2006, for detail). Thus, our approach is similar to modelling performed by Terradas et al. (2007), who studied the excitation of fast magnetoacoustic modes of a plasma cylinder. But, the main emphasis of our work is put on forward modelling of the observational manifestation of the sausage modes. **Modelling of sausage oscillations in terms of the initial value problem, applied in this work, is adequate to the aim of the study: to study the observational manifestation of the response of a coronal loop to an impulsive axisymmetric excitation. As in thick and dense flaring loops the ratio of the minor radii to the lengths is rather large, the analytical results obtained in the thin flux tube approximation are not quantitatively applicable.**

This paper is organised as follows. The analytical model and numerical methods are described in Sect. 2. Numerical results are presented and discussed in Sect. 3, and the observability of the sausage mode is discussed in Sect 4. This paper is concluded by a summary of the main results in Sect. 5.

2. Numerical setup

To model a sausage oscillation of a plasma cylinder we used the ideal magnetohydrodynamic (MHD) equations:

$$\frac{\partial \varrho}{\partial t} + \nabla \cdot (\varrho \mathbf{V}) = 0, \qquad (1)$$

$$\varrho\frac{\partial \mathbf{V}}{\partial t} + \varrho(\mathbf{V}\cdot\nabla)\mathbf{V} = -\nabla p + \frac{1}{\mu}(\nabla\times\mathbf{B})\times\mathbf{B}, \quad (2)$$

$$\frac{\partial \mathbf{B}}{\partial t} = \nabla\times(\mathbf{V}\times\mathbf{B}), \quad (3)$$

$$\frac{\partial p}{\partial t} + \mathbf{V}\cdot\nabla p = -\gamma p\nabla\cdot\mathbf{V}, \quad (4)$$

$$\nabla\cdot\mathbf{B} = 0, \quad (5)$$

where ϱ is the mass density, p is the gas pressure, $\mathbf{B}$ is the magnetic field, $\mathbf{V} = [V_\mathbf{x}, V_\mathbf{y}, V_\mathbf{z}]$ is the flow velocity, μ is the magnetic permeability and $\gamma = 5/3$ is the ratio of specific heats. In this study we ignore the effects of gravity, field-line curvature and twist.

We model a coronal loop as a straight magnetic cylinder. The equilibrium density profile is given by the Gaussian function:

$$\varrho(x,y) = (\varrho_i - \varrho_e)\exp\left(-\frac{x^2+y^2}{2w^2}\right) + \varrho_e, \quad (6)$$

where ϱ_i is the density at the loop centre, ϱ_e is the density of the ambient medium far from the loop, and w is the half-width of the Gaussian function. The equilibrium magnetic field is uniform in the z-direction, but in the transverse direction is given by the following profile:

$$B_z(x,y) = (B_i - B_e)\exp\left(-\frac{x^2+y^2}{2w^2}\right) + B_e. \quad (7)$$

The internal value of the magnetic field B_i was lower than the external value B_e. We assume that initially the cylinder is in the pressure balance with the surrounding plasma, and at the beginning the plasma flows are zero in the simulation region. To maintain the total pressure balance between the cylinder and surrounding plasma we choose the gas pressure within the cylinder according to the condition:

$$p_i = \frac{1}{2\mu}(B_e^2 - B_i^2) + p_e. \quad (8)$$

The Alfvén speed outside the cylinder is higher than inside it, which is the necessary condition for the existence of the trapped modes.

Eqs. (1-5) are numerically solved with the use of the Lagrangian-remap code Lare3d (Arber et al. 2001). In our studies we simulate the plasma dynamics in a domain $(-10,10)\times(-10,10)\times(0,7)$ Mm covered by $400\times400\times100$ grid points. We performed grid convergence studies to check the numerical results. At the footpoints of the cylinder we implemented line-tying boundary condition to mimic the dense layer of the solar atmosphere. Elsewhere we set zero gradients boundary conditions. The specific spatial scales shown above are given just for reference, and can be readily changed by re-normalisation.

To excite a sausage mode we used a pulse in the transverse components of the velocity:

$$V_{\mathrm{x}0} = Ax\exp\left(-\frac{x^2+y^2}{2w^2}\right)\sin(kz), \quad (9)$$

$$V_{\mathrm{y}0} = Ay\exp\left(-\frac{x^2+y^2}{2w^2}\right)\sin(kz), \quad (10)$$

where $k = \pi N/L_0$ is the longitudinal wave number with N being the longitudinal mode number, and A is an initial amplitude, and L_0 is the length of the cylinder. Choosing different values of the integer N, we excite different standing longitudinal harmonics, with the lowest being in the leaky regime. To avoid nonlinear effects we set $A = 0.01\ C_{Ae}$. For small values of β this amplitude can be comparable with the sound speed. However, as for small β the sausage mode is essentially transverse, it is mainly determined by the values of the Alfvén speed in the equilibrium, which was confirmed by our experiments.

In all our experiments the ratio of the cylinder width w to its length was kept constant, 2/7. In different experiments we changed the density contrast between the internal and external plasmas from 2 to 10. The ratio of the internal and external values of the magnetic field was kept constant, 0.89. The difference between the temperatures of the internal and external plasmas was varied to keep the total pressure balance. The value of plasma-β was always lower than 0.3. Hence, in our experiments we studied plasma cylinders with the ratio of the external and internal Alfvén speeds from 1.41 to 3.16.

3. Spatial structure and periods of sausage modes

We performed a series of numerical experiments simulating the sausage mode in the magnetic cylinder. For this, we excite perturbations of the equilibrium configuration, induced by the pulse described in the previous section. The initial perturbation develops into a trapped or leaky global sausage mode oscillation, depending upon the excited longitudinal harmonic (as the ratio of the longitudinal wavelength to the width of the cylinder for different harmonics is either greater or smaller than the cut-off value). Figure 1 shows contour-plots of the perturbations of the mass density ϱ, the longitudinal component of the magnetic field B_z, a transverse component of the velocity V_y and the longitudinal component of the velocity V_z in the plane $y = 0$ at the time $t = 3w/C_{Ae}$ for the 5-th harmonic of the sausage mode. It is clearly visible that the axis of the cylinder is not perturbed. Perturbations of the mass density and magnetic field are in phase while the radius of the cylinder is perturbed in anti-phase with the density and magnetic field. Due to the finite value of plasma-β (the maximum value in the cylinder is $\beta = 0.3$) longitudinal flows are present in the cylinder, but its amplitude is about an order of magnitude smaller than for the transverse flows.

Figure 2 shows a snapshot of the profile of the perturbation of density versus the transverse coordinate x in a sausage mode, obtained from the simulation (the blue curve). We can see that the mode rearranges the plasma in the cylinder in the transverse direction, causing the density enhancements and rarefactions.

Qualitatively, this behaviour is well consistent with the estimates which can be obtained analytically for a plasma slab. In the zero β case, the sausage eigenfunctions (Cooper et al. 2003b) which describe the perturbation of the transverse component of the plasma velocity in the sausage mode in a slab with the symmetric Epstein profile of the density are given by the expression:

$$\tilde{V}_x = \frac{\sinh(x/w)}{\cosh(x/w)^\lambda}, \quad (11)$$

where $\lambda = \sqrt{C_{Ae}^2 - C_p^2}|k|w/C_{Ae} + 1$, w is a half-width of the wave-guiding non-uniformity, k is the longitudinal wave number and C_p is the phase speed, determined from the

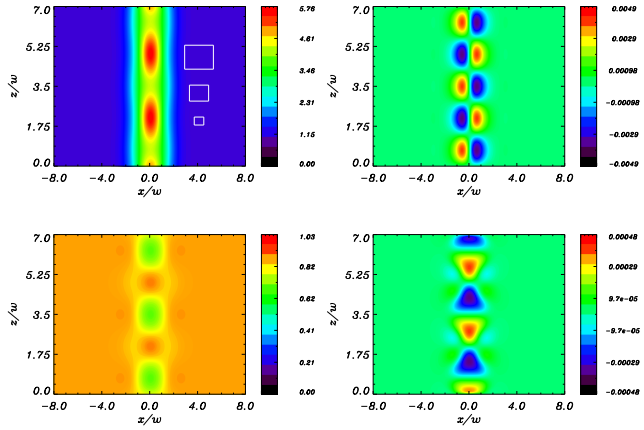

Fig. 1. Snapshots of the perturbations of the physical parameters in a plasma cylinder at $t = 3$ (the time is normalised to w/C_{Ae}): the mass density ϱ (top left panel), the longitudinal component of the magnetic field B_z (bottom left panel), the transverse component of the velocity, V_y, (top right panel) and the longitudinal component of the velocity V_z (bottom right panel). The spatial coordinates are measured in units of w that is the half width of the cylinder.

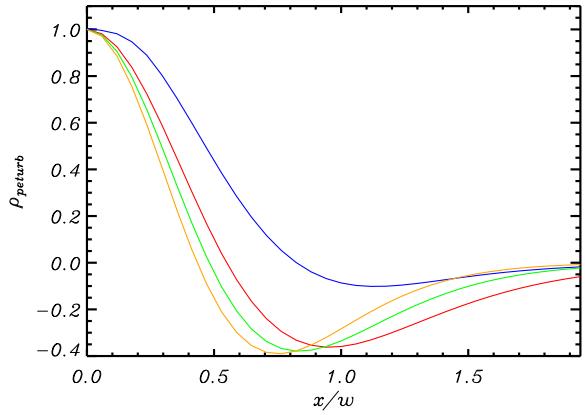

Fig. 2. Snapshots of the density perturbation as a function of the radial coordinate. The blue line corresponds to the result obtained by simulations for a plasma cylinder, and other curves show the analytical results obtained for a plasma slab with the symmetric Epstein profile of the density: the red line for $\lambda = 2$, the green line for $\lambda = 3$ and the orange line for $\lambda = 4$, respectively.

dispersion relation:

$$\frac{|k|w}{C_{Ai}^2}\left(C_p^2 - C_{Ai}^2\right) - \frac{2}{|k|w} = \frac{3}{C_{Ae}}\sqrt{C_{Ae}^2 - C_p^2}. \tag{12}$$

From the continuity equation we obtain the expression which links the perturbation of the density with the transverse velocity:

$$\varrho_{\rm pert} = -\int \frac{\partial\left(\varrho_0 \tilde{V}_x\right)}{\partial x} dt. \tag{13}$$

Substituting (11) to (13) and assuming that the equilibrium density profile is given by the symmetric Epstein profile:

$$\varrho_0(x) = (\varrho_i - \varrho_e)\,\mathrm{sech}^2(x/w) + \varrho_e, \tag{14}$$

where ϱ_i is the density at the loop apex, ϱ_e is the external density, we obtain the profile of the perturbed density. Results obtained for different values of the parameter λ are shown in Fig. 2, and are similar to the structure of the perturbations in our numerical experiments. Thus, in a low-β environment, the plasma is redistributed mainly in the transverse direction, while the total mass of a certain cross-section remains almost the same (and exactly the same in the zero-β case).

Figure 3 shows two typical scenarios of the time evolution of the sausage modes: the trapped (top panel) and leaky (bottom panel) regimes. The trapped mode corresponds to the fifth longitudinal harmonic and the leaky mode to the first harmonic. Hence their wavelengths are either greater or smaller than the cutoff wavelength, respectively. The signal shown is the perturbation of the longitudinal component of magnetic field, B_z, at the centre of cylinder. Because of their symmetry both excited modes have the maximum perturbation of this physical quantity there. The signal corresponding to the trapped mode is almost harmonic and decay-less. The apparent variations of its amplitude are caused by some minor contamination of the signal by other harmonics which are excited because of the mismatch between the initial excitation and the spatial structure of the fifth longitudinal harmonics. In the leaky regime we see that the oscillation is also harmonic, but quickly decaying in time. The decay is associated with the radiation of the fast magnetoacoustic waves in the external medium. The efficiency of the leakage is determined by the ratio of the longitudinal wavelength and the cutoff wavelength. In physical terms, for a fixed wavelength and the diameter of the cylinder, the leakage is more efficient for a lower ratio of the internal and external densities. In Fig. 3 we illustrate this effect by showing the time behaviour of the leaky mode for two values of the density contrast, $\varrho_i/\varrho_e = 10$ (black line) and $\varrho_i/\varrho_e = 5$ (red line). It is evident that leaky sausage oscillations are damped more slowly in a denser cylinder. These results are in an agreement with Cally (1986, 2003); Smith et al. (1997); Nakariakov et al. (2003); Terradas et al. (2005) who showed that the wave leakage is weaker in a denser loop. Also, there is a certain indication of the presence of the transient shorter period oscillations, **which may be connected with the higher leaky harmonics (Cally 1986, 2003)**. These modes decay very quickly and are hardly detectable in real data in the presence of noise.

Following Pascoe et al. (2007b); Inglis et al. (2009) we studied the dependence of the period of sausage oscillations upon the wavelength, covering both trapped and leaky regimes. Figure 4 shows the dependence for different density contrast ratios. Different wavelengths were taken as different harmonics of the standing sausage mode. To estimate the period we collected the time dependence of the longitudinal component of the magnetic field B_z at the centre of the cylinder, and fitted the obtained oscillatory curve with a sine-function:

$$D(t) = D_0 + D_1 \sin\left(D_2 t + D_3\right) \tag{15}$$

by the method of least squares. A similar result could be obtained with the use of the Fourier transform, but in the case of the oscillations with low quality, e.g. in the leaky regime, the spectral analysis with the use of the best-fitting technique is more preferable. The period of oscillations is

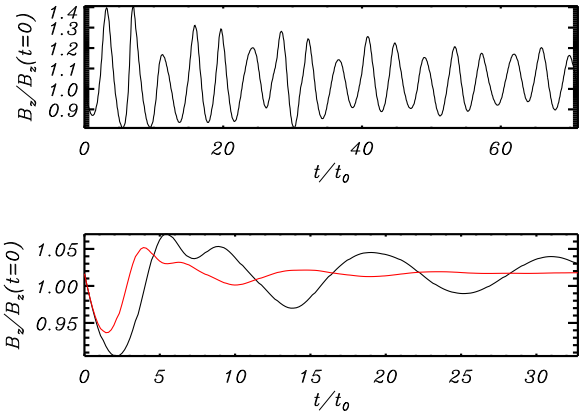

Fig. 3. Time dependence of the longitudinal component of the magnetic field, B_z at the centre of the cylinder for the fifth (top panel) and first (bottom panel) longitudinal harmonics of the sausage mode, corresponding to trapped and leaky modes respectively. The black curve in the bottom panel corresponds to the density contrast of 10, and the red curve to 5.

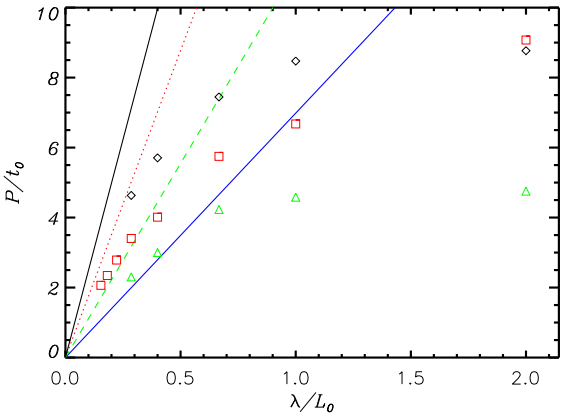

Fig. 4. The dependence of the period of sausage modes upon the wavelength for different density contrast ratios: 2 (triangle), 5 (square) and 10 (diamonds). The lowest blue (solid) line shows the cutoff value $2L/C_{Ae}$. The green (dashed), red (dotted) and upper black (solid) lines correspond to the values of $2L/C_{Ai}$ for density contrast ratios of 2, 5 and 10 respectively. The period is measured in the units $t_0 = w/C_{Ae}$.

then obtained as $P = 2\pi/D_2$. The periods of the trapped modes are situated between the straight lines $2L/C_{Ai}$ and $2L/C_{Ae}$. In the leaky regime, the periods lie below the line $2L/C_{Ae}$, but increase with the increase in the wavelength. Hence, sausage modes of longer wavelengths have longer periods in both trapped and leaky regimes. We would like to point out that in the highly leaky regime the determination of the period has intrinsic difficulties, connected with the very rapid decay of the oscillation. Hence, the rightmost points in Fig. 4 should be taken with caution.

4. Manifestation of sausage modes in observations

The sausage mode is essentially compressible, producing modulation of the density of the plasma and the absolute value of the magnetic field. On the other hand, in a low-β plasma, this mode is also essentially transverse, causing

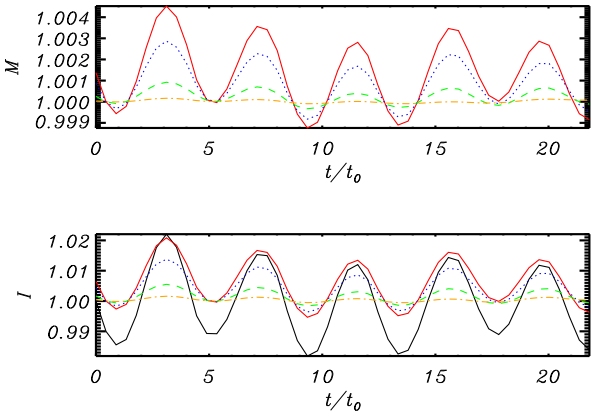

Fig. 5. The time dependence of the LOS-integrated mass $\mathcal{M}$ (top panel) and emission intensity $\mathcal{I}$ (bottom panel) in a sausage-oscillating cylinder for different "widths" of the LOS (pixel sizes). In all the cases the LOS is directed across the cylinder and passes through its centre. The red (solid) lines correspond to an infinitely thin line-of-sight, the blue (dotted) lines correspond to the pixel with the size of the half width of the cylinder w, the green (dashed) lines to $2w$ and the orange (dashed-dotted) lines to $3w$ lines, respectively. The black solid line in the bottom panel shows the relative variation of the density at the centre of the cylinder. The time is measured in the units $t_0 = w/C_{Ae}$.

plasma flows mainly in the direction perpendicular to the magnetic field. Often, from the essential compressibility of this mode it is deduced that it must be responsible for significant perturbations of the intensity of the emission generated in the oscillating object. However, as it was pointed out in (Cooper et al. 2003a), manifestation of MHD modes in observations in the optically thin regime is also significantly affected by the effects of the line-of-sight (LOS) integration: the change of the column depth of the waveguide, along the LOS, by the mode. In particular, the importance of this effect for the sausage mode arguably observed in the modulation of gyrosynchrotron emission, has recently been pointed out by Fleishman et al. (2008). Consider the role of the LOS-integration effect for the thermal emission.

In the zero-β regime, the sausage mode moves the plasma in the direction across the magnetic field only (see, e.g., the formalism developed in Cooper et al. 2003b). Hence, according to the mass conservation law, the mass of a transverse cross-section of the oscillating cylinder should remain always constant during the oscillation. If one probes the mass in the cylinder, integrating the mass density along an infinitely thin LOS, the "LOS mass" would vary in time, as the plasma moves not only along the LOS but also sideways. On the other hand, if the "width" of the LOS (in other words, the pixel size or the half-width of the point spread function) is larger than the diameter of the waveguiding cylinder, the displaced mass would always be in the region of the integration and hence the integral remains constant in all phases of the oscillation cycle.

This effect is illustrated by Fig. 5. Using results of the numerical simulations described in Section 3 we estimated the line integral of the density along the x-axis at the centre

of the cylinder:

$$\mathcal{M}(t) = \int_{(\mathrm{LOS})} \varrho(\mathbf{r}, t) dx \tag{16}$$

for different "widths" of the LOS. The specific value of the LOS width was controlled by the number of the computational grid points, and was measured in the units of the equilibrium width w of the cylinder. The pixels of the different sizes, used in the calculations, are shown in the top left panel of Fig. 1. It is evident from Fig. 5 that for sufficiently large pixels, perturbations of the LOS-integrated mass tends to zero.

In the optically thin regime, thermal emission is proportional to the density squared. Hence, the emission intensity can be estimated as:

$$\mathcal{I}(t) = \int_{(\mathrm{LOS})} \varrho^2(\mathbf{r}, t) dx. \tag{17}$$

The time variation of the emission intensity for different sizes of the pixel are shown in the bottom panel of Fig. 5. For reference, we give the relative perturbation of the density at the centre of the cylinder. It is evident that the increase in the pixel size leads to the sharp decrease in the relative amplitude of the emission intensity, similarly to the case of the LOS-integrated mass. It can be readily understood: indeed, for perturbations of a weak amplitude, the relative density squared can be taken as:

$$\int_{(\mathrm{LOS})} \varrho^2 dx = \int_{(\mathrm{LOS})} (\varrho_0 + \varrho_{\mathrm{pert}})^2 dx = \tag{18}$$

$$\int_{(\mathrm{LOS})} (\varrho_0^2 + 2\varrho_0 \varrho_{\mathrm{pert}} + \varrho_{\mathrm{pert}}^2) dx. \tag{19}$$

For large pixels, the time variation of the LOS integral occurs only because of the third term in the integrand on the right hand side of Eq. (19). Hence, the time variation of the intensity is quadratically proportional to the density perturbation and is negligibly small.

5. Summary and discussion

We have performed a parametric study of fast magnetoacoustic oscillations of a thick and dense coronal loop, modelled by a plasma cylinder embedded in a plasma with different properties and penetrated by straight magnetic field, **emphasising their observational manifestation**. The oscillations of the sausage symmetry (with the azimuthal wave number $m = 0$) were considered only. The plasma both inside and outside the cylinder was taken of low-β. The transverse profile of the plasma density was smooth, without steep gradients or discontinuities. The oscillations were impulsively excited and then simulated with the use of the full set of ideal MHD equations. Oscillations with low amplitudes were considered only.

We summarise our findings as following:

1. The behaviour of short-wavelength sausage oscillations of a plasma cylinder is well consistent with the analytical results obtained for a cylinder with the step-function profile and smooth plasma slab (Zaitsev & Stepanov 1975; Edwin & Roberts 1983; Roberts et al. 1984; Cooper et al. 2003b). The oscillations are trapped in the cylinder, their phase speed has a value between the Alfvén speed inside and outside the cylinder, and their period is determined by the ratio of the phase speed and the wavelength. Sausage waves are essentially compressible, perturbing the density of the plasma and the absolute value of the magnetic field, and transverse, moving the plasma in the direction across the field.
2. Sausage oscillations of the wavelengths longer than the cutoff value are leaky. The attenuation of the oscillations depends on the density contrast between the cylinder and the ambient medium, **which is consistent with the analytical prediction made in Cally (1986, 2003)**. For the plasma parameters typical for coronal plasma structures, e.g. dense plasma loops, the damping time can be of several periods of the oscillations. Thus, long-wavelength sausage modes can last for sufficiently long time to be detected in observations.
3. The period of leaky sausage modes is longer than the period of trapped sausage modes, **and in thick and dense flaring loops** is determined by the ratio of the Alfvén speed outside the cylinder and the wavelength (for the fundamental or global mode it is double the length of the plasma cylinder). This is consistent with the results obtained for a smooth plasma slab (Pascoe et al. 2007b; Inglis et al. 2009). In particular, this result confirms the qualitative conclusion made by Nakariakov et al. (2003) and Aschwanden et al. (2004) that the period of global sausage modes **observed in the gyrosynchrotron emission generated in flaring loops** is determined by the length of the loop, not by its radius. **On the other hand, the dependence of the period of sausage oscillations on the wavelength in the leaky regime shows some saturation. It may be consistent with the independence of the period on the wavelength, found by (Zaitsev & Stepanov 1975; Cally 1986; Kopylova et al. 2007) in the thin flux tube approximation, when the ratio of the radius of the cylinder to the wavelength tends to zero. This topic deserves a detailed dedicated study.**
4. The observational manifestation of sausage oscillations in the thermal emission, proportional to the density of the emitting plasma squared, depends upon whether the oscillating plasma non-uniformity is spatially resolved or not. If the pixel size or the half-width of the spread function are about the width of the non-uniformity, the perturbation of the emission intensity by sausage oscillations is proportional to the relative amplitude squared. For example for an oscillation of the amplitude 5%, the observed amplitude of the intensity variation is only 0.25%. This effect should be taken into account in distinguishing between the sausage oscillations and, e.g., torsional oscillations, which both produce periodic non-thermal broadening of the emission lines by the Doppler shift.

We conclude that the sausage mode is a good tool for the seismological probing of the plasma in oscillating coronal plasma non-uniformities, giving us the information about the Alfvén speed inside and outside the non-uniformity. The observational manifestation of this mode is very much affected by the LOS-integration effect and by the pixel size, and it has to be taken into account in the data analysis.

Acknowledgements MG is supported by the Newton International Fellowship NF090143. TVD has received

funding from the Odysseus programme of the FWO-Vlaanderen and from the EU's Framework Programme 7 as an ERG with grant number 276808.

References

Arber, T. D., Longbottom, A. W., Gerrard, C. L., & Milne, A. M. 2001, Journal of Computational Physics, 171, 151
Aschwanden, M. J., Nakariakov, V. M., & Melnikov, V. F. 2004, ApJ, 600, 458
Brown, J. C. & Hoyng, P. 1975, ApJ, 200, 734
Cally, P. S. 1986, Sol. Phys., 103, 277
Cally, P. S. 2003, Sol. Phys., 217, 95
Cooper, F. C., Nakariakov, V. M., & Tsiklauri, D. 2003a, A&A, 397, 765
Cooper, F. C., Nakariakov, V. M., & Williams, D. R. 2003b, A&A, 409, 325
Díaz, A. J., Oliver, R., Ballester, J. L., & Roberts, B. 2004, A&A, 424, 1055
Edwin, P. M. & Roberts, B. 1982, Sol. Phys., 76, 239
Edwin, P. M. & Roberts, B. 1983, Sol. Phys., 88, 179
Fleishman, G. D., Bastian, T. S., & Gary, D. E. 2008, ApJ, 684, 1433
Fujimura, D. & Tsuneta, S. 2009, ApJ, 702, 1443
Inglis, A. R., Nakariakov, V. M., & Melnikov, V. F. 2008, A&A, 487, 1147
Inglis, A. R., Van Doorsselaere, T., Brady, C. S., & Nakariakov, V. M. 2009, A&A, 503, 569
Kopylova, Y. G., Melnikov, A. V., Stepanov, A. V., Tsap, Y. T., & Goldvarg, T. B. 2007, Astronomy Letters, 33, 706
Melnikov, V. F., Reznikova, V. E., Shibasaki, K., & Nakariakov, V. M. 2005, A&A, 439, 727
Nakariakov, V. M., Melnikov, V. F., & Reznikova, V. E. 2003, A&A, 412, L7
Nakariakov, V. M. & Verwichte, E. 2005, Living Reviews in Solar Physics, 2, 3
Pascoe, D. J., Nakariakov, V. M., & Arber, T. D. 2007a, Sol. Phys., 246, 165
Pascoe, D. J., Nakariakov, V. M., & Arber, T. D. 2007b, A&A, 461, 1149
Pascoe, D. J., Nakariakov, V. M., Arber, T. D., & Murawski, K. 2009, A&A, 494, 1119
Roberts, B., Edwin, P. M., & Benz, A. O. 1984, ApJ, 279, 857
Rosenberg, H. 1970, A&A, 9, 159
Ruderman, M. S. & Roberts, B. 2006, Sol. Phys., 237, 119
Smith, J. M., Roberts, B., & Oliver, R. 1997, A&A, 317, 752
Srivastava, A. K., Zaqarashvili, T. V., Uddin, W., Dwivedi, B. N., & Kumar, P. 2008, MNRAS, 388, 1899
Terradas, J., Andries, J., & Goossens, M. 2007, Sol. Phys., 246, 231
Terradas, J., Oliver, R., & Ballester, J. L. 2005, A&A, 441, 371
Van Doorsselaere, T., De Groof, A., Zender, J., Berghmans, D., & Goossens, M. 2011, ApJ, 740, 90
Verwichte, E., Foullon, C., & Nakariakov, V. M. 2006, A&A, 449, 769
Zaitsev, V. V. & Stepanov, A. V. 1975, A&A, 45, 135
Zaitsev, V. V. & Stepanov, A. V. 1982, Soviet Astronomy Letters, 8, 132